

Copper Corrosion Protection of Various Silane-Modified Poly(vinyl imidazole)(1)s

HYUNCHEOL KIM, JYONGSIK JANG

Department of Chemical Technology, Seoul National University, San 56-1, Shinlimdong Kwanakgu, Seoul, South Korea

Received 14 May 1996; accepted 24 October 1996

ABSTRACT: Vinyl imidazole (VI) was copolymerized with four silane coupling agents, allyl trimethoxysilane (ATS), γ -methacryloxypropyl trimethoxysilane (MPS), 3(*N*-styrylmethoxyl-2-amino-ethylamino)propyltrimethoxysilane hydrochloride (STS), and vinyl trimethoxysilane (VTS), in benzene at 68°C using azobisisobutyronitrile (AIBN) as an initiator. Fourier transform infrared reflection and absorption spectroscopy (FTIR-RAS) and scanning electron microscopy (SEM) were applied to the study of the corrosion protection on copper by various silane-modified poly(vinyl imidazole)(1)s [PVI(1)]s. Four silane-modified PVI(1)s proved to be good corrosion inhibitors in humid conditions. However, the corrosion protection capability at an elevated temperature of silane-modified PVI(1)s depended on their thermal stability. Poly(VI-co-VTS) showed the best corrosion protection capability at elevated temperature due to its highest thermal stability. © 1997 John Wiley & Sons, Inc. *J Appl Polym Sci* **64**: 2585–2595, 1997

Key words: silane modified PVI(1)s; copper corrosion protection; thermal stability

INTRODUCTION

Corrosion protection for metal by organic coatings is well known as the cost-effective and flexible mean. In the copper industry, the development of new corrosion inhibitors has been constantly demanded for its wide application. Imidazole and its derivatives are known as good corrosion inhibitors for copper.^{1–11} Especially, it was reported that silane-modified poly(vinyl imidazole)(1) [PVI(1)] was an effective corrosion inhibitor for copper at elevated temperature and in humid conditions.^{12,13}

The role of a silane coupling agent in silane-modified PVI(1) is that of forming chemical bonding with a copper surface to improve the adhesion between copper and the coated copolymer and to exclude water molecules at the copper/copolymer interface. Jang and Ishida reported that silane-modified PVI(1) suppressed copper corrosion at

360°C for 15 min in air and at 80°C with 100% relative humidity for 24 h, and that copolymer degradation was responsible for copper corrosion at elevated temperature.^{12,13} Therefore, silane-modified PVI(1) with a higher thermal stability is required for copper corrosion protection at temperatures above 360°C.

In this study, various silane-modified PVI(1)s were synthesized, and the corrosion protection for copper at elevated temperature and in humid conditions was investigated by Fourier transform infrared reflection and absorption spectroscopy (FTIR-RAS) and scanning electron microscopy (SEM). In addition, the relationship between corrosion protection capability and thermal stability of various silane-modified PVI(1)s was studied.

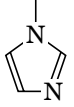
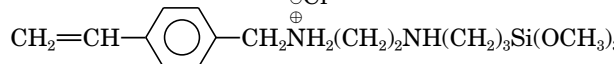
EXPERIMENTAL

Vinyl imidazole (VI) and vinyl trimethoxysilane (VTS) were purchased from Aldrich Chemical Co., and allyl trimethoxysilane (ATS), γ -methacryloxy-

Correspondence to: J. Jang.

© 1997 John Wiley & Sons, Inc. CCC 0021-8995/97/132585-11

Table I The Chemical Structures of Monomers

Monomers	Chemical Structures
VI	$\text{CH}_2=\text{CH}$ 
VTS	$\text{CH}_2=\text{CHSi}(\text{OCH}_3)_3$
ATS	$\text{CH}_2=\text{CHCH}_2\text{Si}(\text{OCH}_3)_3$
γ -MPS	$\text{CH}_2=\text{C}(\text{CH}_3)\text{COO}(\text{CH}_2)_3\text{Si}(\text{OCH}_3)_3$
STS	$\text{CH}_2=\text{CH}-\text{C}_6\text{H}_4-\text{CH}_2\text{NH}_2^+(\text{CH}_2)_2\text{NH}^+(\text{CH}_2)_3\text{Si}(\text{OCH}_3)_3 \text{Cl}^-$ 

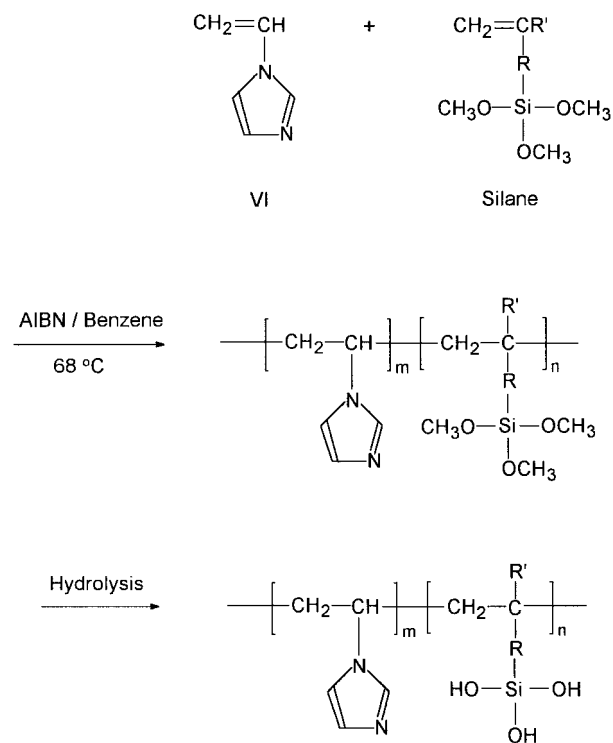
propyl trimethoxysilane (MPS), and 3(*N*-styryl-methoxyl-2-amino-ethylamino)propyltrimethoxysilane hydrochloride (STS), from Petrach Systems. All monomers except STS were distilled *in vacuo* to yield pure and colorless liquids. STS was used without distillation. AIBN from Wako Pure Chemical Industries was dissolved in warm methanol (35°C), recrystallized in an ice bath, then dried in a vacuum oven at room temperature for 2 days.

Four silane-modified PVI(1)s were synthesized by free-radical copolymerization using azobisisobutyronitrile (AIBN) as an initiator. VI was respectively copolymerized with four silane coupling agents for 24 h in benzene at 68°C with stirring in an argon atmosphere. In each case, the total monomer concentration was 1M, and the initiator concentration was fixed at 1×10^{-3} M. The mole ratios of the two monomers in the feed were 1 : 1. The chemical structures of monomers are represented in Table I. As the side-chain length of silane coupling agents grows longer, the siloxane bond number per weight becomes higher. The siloxane bond number per weight is defined as the ratio of the number of the Si—O bonds to molecular weight. Thermal stability of silane-modified PVI(1)s is influenced by the siloxane bond number per weight. A schematic diagram of copolymerization and hydrolysis is shown in Figure 1.

To induce chemical bonding between the copper surface and silane-modified PVI(1)s, their partial hydrolysis was carried out for 1 h using a mixed solvent of ethanol/benzene with pH 7. The partially hydrolyzed solution was cast onto copper plates with a microsyringe; then, the samples were dried at 30°C for 12 h in air to remove the solvent in the copolymer film. Copper plates (1.2

$\times 5.0 \times 0.3$ cm) were mechanically polished with No. 5 chromic oxide, washed with *n*-hexane and ethanol in an ultrasonic bath, rinsed with a 1% HCl/distilled water solution, distilled water, and ethanol, and then dried with a stream of nitrogen gas.^{12,13}

Film thickness was calculated based on the concentration of the copolymer solution, the copolymer density, and the area of the copper surface. In this study, the thickness of copolymer films on copper plates was fixed as 2 μm .

**Figure 1** Schematic diagram of copolymerization and hydrolysis.

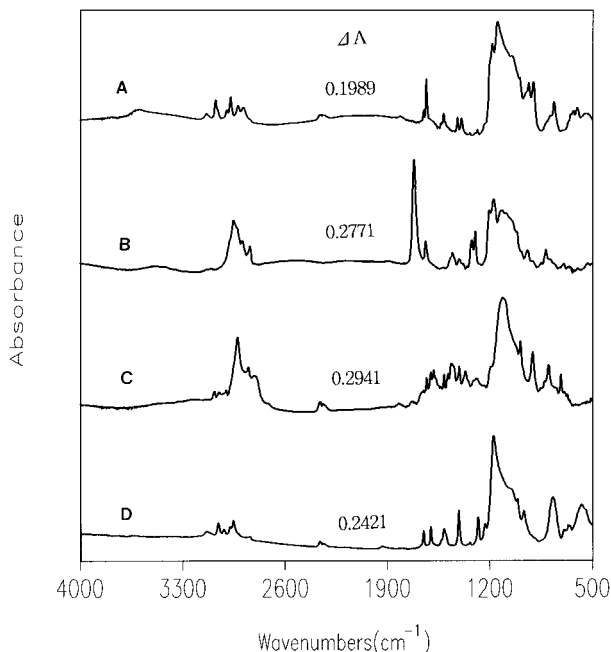


Figure 2 FTIR reflection and absorption spectra of the copolymer films coated on copper plates: (A) poly(ATS-co-VI); (B) poly(γ -MPS-co-VI); (C) poly(STS-co-VI); (D) poly(VI-co-VTS).

FTIR-RAS was used to characterize the copolymer films coated onto the copper surface. The spectrometer was continuously purged with nitrogen gas to remove water vapor and the atmospheric CO_2 . Absorbance spectra were obtained using a Bomem MB-100 spectrometer at a resolution of 4 cm^{-1} ; 64 scans were collected. A Graseby Specac P/N 19650 monolayer/grazing angle accessory was used. The angle of incidence was 78° and a freshly polished copper plate was used to obtain the reference spectrum. In addition, FTIR transmission spectroscopy was used to characterize the copolymer films coated on KBr pellets.

An adhesion test (ASTM D3359-83 tape test) was performed to investigate the adhesion strength between the copper surface and the thermally degraded copolymer using adhesion tape. A Scotch tape test is composed of applying and briskly lifting the tape over cuts made in the film. This tape test is used to assess the adhesion of coated polymer on a metal surface, but it does not classify the coating materials of high adhesion strength.

SEM was used to observe the surface morphology of the copolymer-coated copper surface. The instrument used was a JEOL JSM-35 scanning microscope. Specimens were coated with a thin layer of gold to eliminate charging effects.

RESULTS AND DISCUSSION

FTIR reflection and absorption spectra of the copolymer films coated on copper plates are demonstrated in Figure 2. The peaks in the $3000\text{--}2800 \text{ cm}^{-1}$ regions result from Si-O-CH_3 , which means that the copolymers are not completely hydrolyzed in this experimental condition. The strong broad bands in the $1300\text{--}900 \text{ cm}^{-1}$ regions are caused by the Si-O-Si and Si-O-CH_3 functional groups and the imidazole ring. The relative peak intensity in the $1300\text{--}900 \text{ cm}^{-1}$ regions is the strongest in Figure 2(D) because it has the highest siloxane bond number per weight.

Figure 3 shows FTIR reflection and absorption spectra of a bare copper plate heated at 360°C in air. The extent of cuprous oxide formation on the copper surface depends on the heat treatment time. As shown in Figure 3(B) and (C), the cuprous oxide appears as a doublet at 655 and 608 cm^{-1} . The peak at 655 cm^{-1} corresponds to the longitudinal optical mode. The peak at 608 cm^{-1} is attributed to the transverse optical mode of the high-frequency phonon, which indicates that the cuprous oxide layer is at least 200 nm in thickness.¹⁴ As the heat treatment time increases, the intensity of the peak at 608 cm^{-1} increases due to

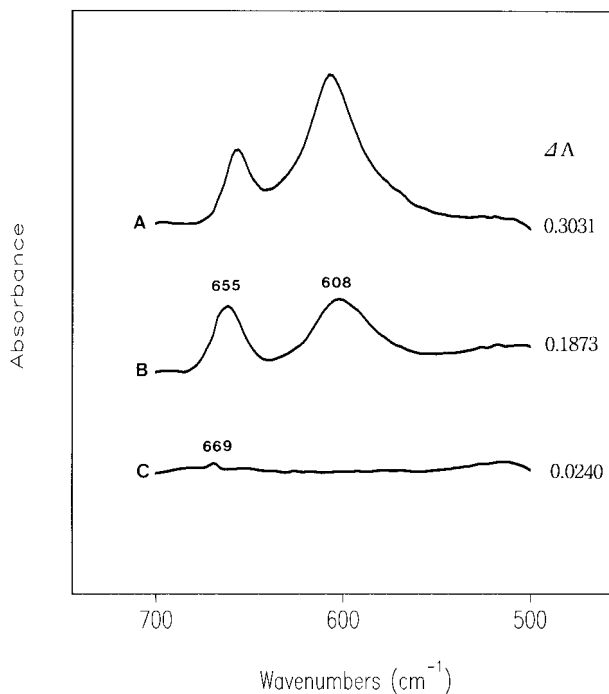


Figure 3 FTIR reflection and absorption spectra of a bare copper plate at 360°C in air: (A) 0 min; (B) 15 min; (C) 30 min.

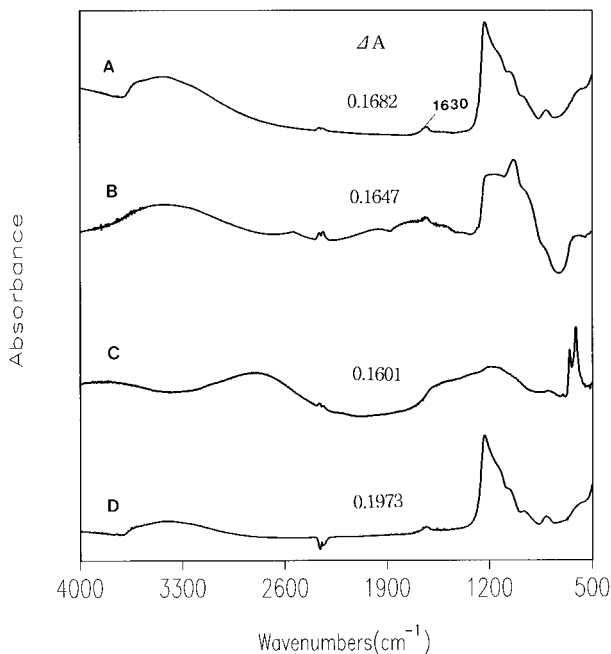


Figure 4 FTIR reflection and absorption spectra of the copolymer films on copper plates heated at 360°C for 15 min: (A) poly(ATS-*co*-VI); (B) poly(γ -MPS-*co*-VI); (C) poly(STS-*co*-VI); (D) poly(VI-*co*-VTS).

the increase in cuprous oxide layer thickness. The peak at 669 cm^{-1} in Figure 3(A) is caused by the atmospheric CO_2 .

To study the corrosion protection capability for copper at elevated temperature, the copolymer films on copper plates were heated in air. Figure 4 shows FTIR reflection and absorption spectra of the copolymer films on copper plates heated at 360°C for 15 min. Judging from these spectra, all the copolymer films heated on copper plates are severely degraded, and most copolymer peaks, which can be observed in Figure 2, disappeared in Figure 4. The strong broad peaks in the 1300–900 cm^{-1} regions are attributed to the thermally stable Si—O—Si linkages and the Si—OH groups,^{15,16} and their relative peak intensities decrease in the order of poly(VI-*co*-VTS), poly(ATS-*co*-VI), poly(γ -MPS-*co*-VI), and poly(STS-*co*-VI), with a decreasing siloxane bond number per weight. This indicates that the thermal stability of the copolymers depends on the length of the side chain in silane coupling agents. The copolymer with the long side chain is more susceptible to thermal degradation due to its low siloxane bond ratio. The existence of the disiloxane linkages suggests that Si—O— CH_3 groups in the copolymers are hydrolyzed and condensed to form disiloxane

linkages during heat treatment.^{17–19} The small peaks at 1630 cm^{-1} are due to the carbonyl groups caused by molecular water trapped in the infinite siloxane network.²⁰ Poly(STS-*co*-VI) shows only a little peak at 1630 cm^{-1} because it has hardly formed the siloxane network structure. From these spectra, it can be concluded that heating in air of the copolymers induces the siloxane network structure formation as well as the copolymer oxidation.

To deeply investigate the cuprous oxide formation on copolymer-coated copper surfaces, the 700–500 cm^{-1} regions of the spectra shown in Figure 4 are indicated in Figure 5. As shown in Figure 5(C), the spectrum of poly(STS-*co*-VI) demonstrates two cuprous oxide peaks at 655 and 611 cm^{-1} , which means that the cuprous oxide layer formed from copper corrosion is at least 200 nm in thickness. However, poly(STS-*co*-VI) is less corroded in comparison with a bare copper because the peak at 611 cm^{-1} is smaller than that at 655 cm^{-1} . Since no original copolymer peak is shown from Figure 4(C) except the peaks related to the siloxane bond, the formation of cuprous oxide on the copper surface coated with poly(STS-*co*-VI) is attributed to its severe thermal degradation. The spectrum of poly(γ -MPS-*co*-VI) shows less thermal degradation in comparison with that

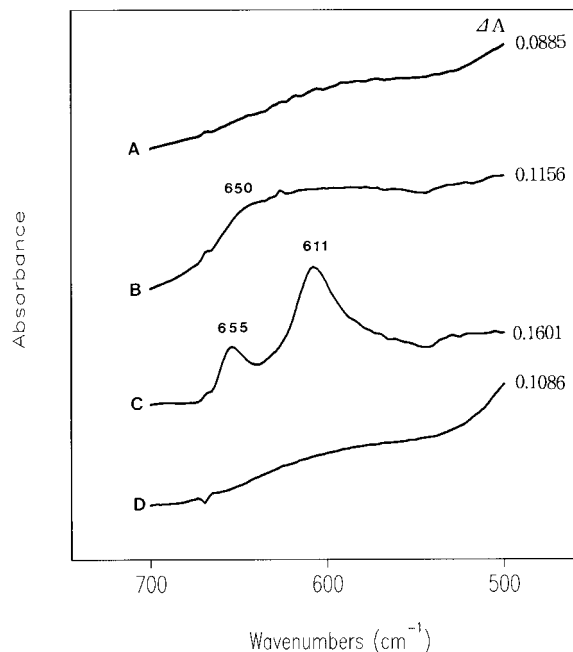


Figure 5 The 700–500 cm^{-1} regions of FTIR reflection and absorption spectra shown in Figure 4: (A) poly(ATS-*co*-VI); (B) poly(γ -MPS-*co*-VI); (C) poly(STS-*co*-VI); (D) poly(VI-*co*-VTS).

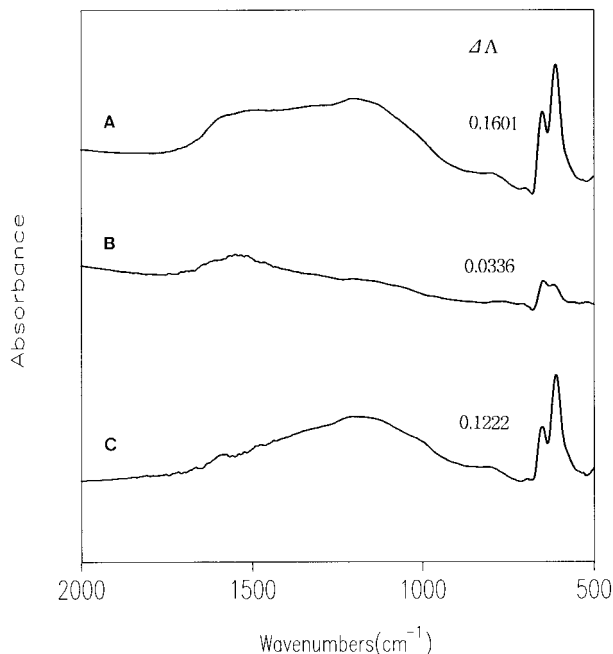


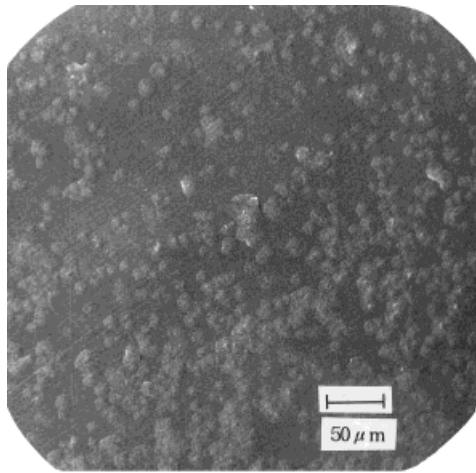
Figure 6 FTIR reflection and absorption spectra of poly(STS-co-VI) before and after adhesion test: (A) copolymer-coated copper surface before adhesion test; (B) flaked copper surface after adhesion test; (C) copolymer flaked off copper surface (spectrum A – spectrum B).

of poly(STS-co-VI) and it shows a weak cuprous oxide peak at 650 cm^{-1} . On the contrary, the other two spectra show no cuprous oxide peak in their spectra in spite of their partial thermal degradation. This means that thermal degradation is not detrimental enough to cause the occurrence of defects in the coated film and that the copper/copolymer interface is still protected from the attack of the air oxygen and water vapor. In this experimental condition, since the other parts of the copolymer except the part related to the siloxane linkage are almost thermally degraded, the corrosion protection capability of each copolymer depends on the siloxane bond number per weight in each copolymer. Since poly(STS-co-VI) with the longest side chain has the lowest siloxane bond number per weight, it is the most susceptible to corrosion at elevated temperature.

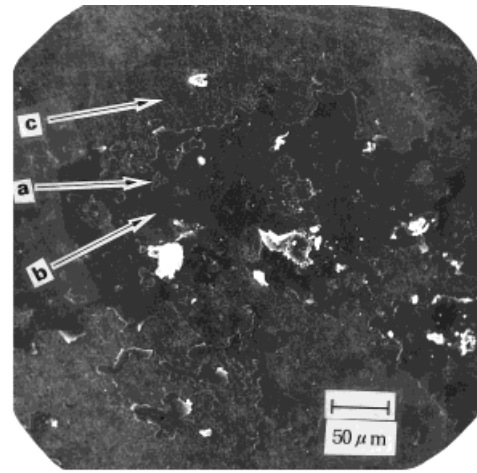
An adhesion test was performed to investigate the adhesion strength between the copper surface and thermally degraded copolymer using adhesion tape. Thermally degraded poly(STS-co-VTS) was flaked off the copper surface due to its poor interfacial adhesion strength. Figure 6 shows FTIR spectra of the copper surface before and after the adhesion tape test. A small copolymer

oxidation peak around 1510 cm^{-1} and cuprous oxide peaks at 655 and 608 cm^{-1} are observed in spectrum B, which means that copolymer oxidation products and cuprous oxide crystals remain on the copper surface after the adhesion tape test. Spectrum C is the subtracted spectrum (spectrum A – spectrum B), which corresponds to the spectrum of the film flaked off the copper surface after the adhesion tape test. From spectra B and C, most copolymer film, which contains some copper oxides, was flaked off the copper surface as a result of the adhesion tape test. This suggests that the interfacial adhesion strength between the copper and the barrier film was weakened by cuprous oxide formation at the copper/copolymer interface and/or that bulk property of barrier film was deteriorated due to its thermal degradation.

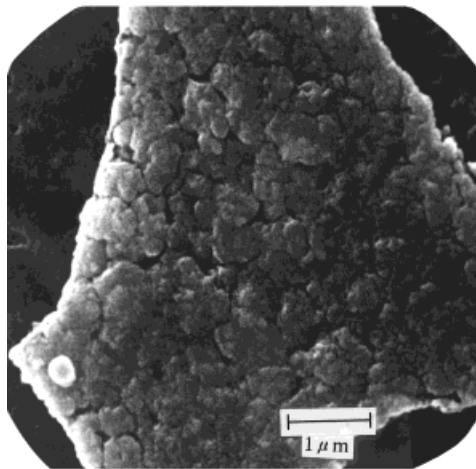
Figure 7 shows scanning electron micrographs of copolymer-coated copper plates at 360°C for 15 min before and after the adhesion tape test. In Figure 7(A), the protruded parts are attributed to the cuprous oxide crystal and the dark background represents the copolymer film. The copper surface [Fig. 7(B)] after the adhesion tape test shows three different regions, whose enlarged parts are shown in Figure 7(C), (D), and (E), respectively. Figure 7(C) shows part of unflaked barrier film, and its surface consists of agglomerates. Figure 7(D) shows the bulk of the barrier film, which results from the cohesive failure of the barrier film. The fracture surface of the barrier film contains micropits with different sizes and small particles. Small particles are copper oxide crystals and small pits represent the empty holes that cuprous oxide crystals have occupied. Figure 7(E) shows a flaked copper surface with copper oxide crystals and small pits. The bright parts represent cuprous oxide crystals on the copper surface. The formation of small pits is because cuprous oxide crystals at the copper/copolymer interface have been separated from the copper surface. This means that the interfacial failure occurred due to cuprous oxide formation at the interface between the copper surface and the barrier film. In addition, film flaked off the copper surface shows also cuprous oxide crystals with an irregular shape [Fig. 7(B)]. This result is good agreement with IR results in Figure 6. Judging from these data, it can be concluded that copper oxide species exist within the barrier film as well as at the copper/copolymer interface. The presence of copper oxide crystals within barrier film suggests that copper diffuses into the barrier film and is oxidized into copper oxide during heat



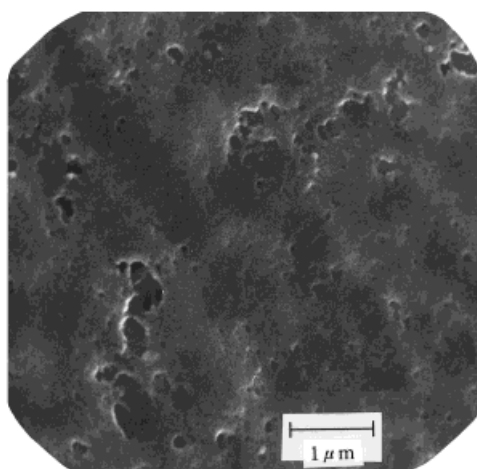
(A)



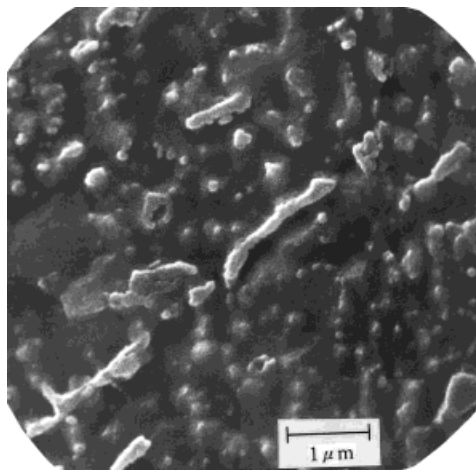
(B)



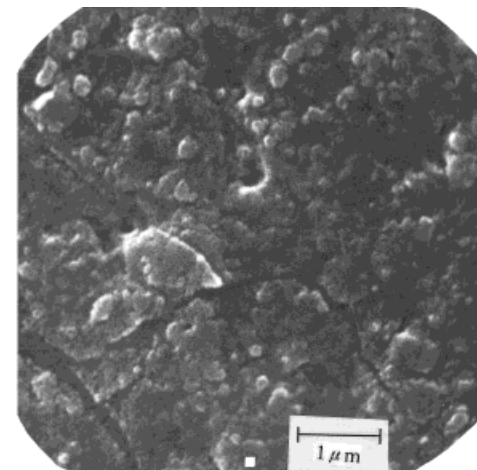
(C)



(D)



(E)



(F)

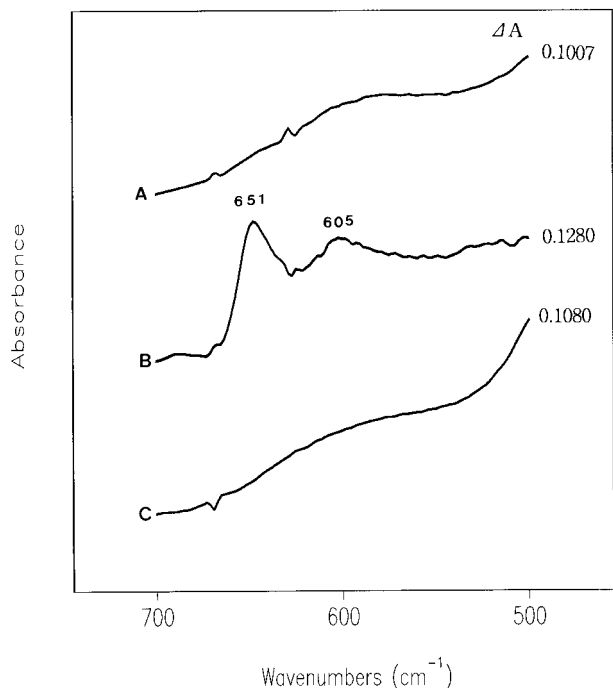


Figure 8 FTIR reflection and absorption spectra of the copolymer films on copper plates heated at 360°C for 30 min: (A) poly(ATS-co-VI); (B) poly(γ -MPS-co-VI); (C) poly(VI-co-VTS).

treatment.^{21,22} On the other hand, the existence of copper oxide crystals at the copper/copolymer interface hints that thermal degradation of the copolymer coated on copper plates causes the occurrence of defects in coated film and allows air oxygen and water vapor to penetrate through the copper/copolymer interface, and so cuprous oxide is formed at the copper/copolymer interface.

Three copolymers except poly(STS-co-VI) were heated at 360°C in air for 30 min. Figure 8 shows FTIR reflection and absorption spectra in the 700–500 cm^{-1} regions of the copolymer films on copper plates heated at 360°C in air for 30 min. The spectrum of poly(γ -MPS-co-VI) shows two cuprous oxide peaks at 651 and 605 cm^{-1} , which means that the formation of copper oxide proceeded conspicuously due to the increased thermal degradation. However, no corrosion peak is yet shown in the spectra of poly(ATS-co-VI) and poly(VI-co-VTS). Two uncorroded samples show

the shiny copper surface in spite of their partial thermal degradation. This implies that poly(ATS-co-VI) and poly(VI-co-VTS) form a thermally stable siloxane network structure through the Si—O—Si linkages due to their high siloxane bond ratio.

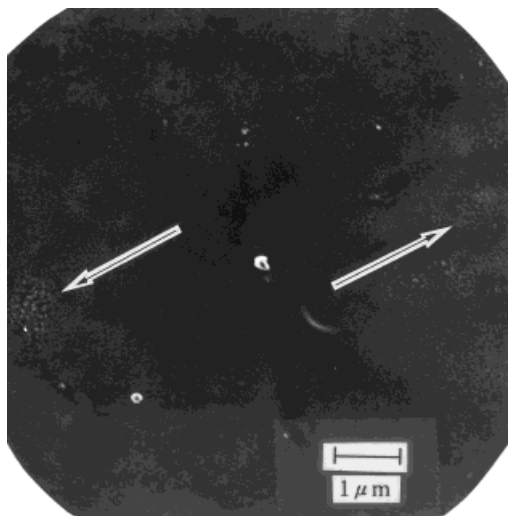
Figure 9 shows scanning electron micrographs of poly(γ -MPS-co-VI) on the copper plate heated at 360°C for 30 min. In Figure 9(A), cuprous oxide crystals, which are indicated by the arrows, are formed on the copolymer-coated copper surface, but are very small in size. This means that film defects are formed, but that cuprous oxide crystals have not fully grown in this condition. Cuprous oxide crystals with a polyhedron shape are observed in Figure 9(B). Prolonged heat treatment induced the growth of cuprous oxide crystals through defects in the barrier film. However, thermally degraded copolymer films were not flaked off the copper surface in the adhesion tape test. This suggests that cuprous oxide is formed through film defects, not at the whole copper/copolymer interface.

Poly(ATS-co-VI) and poly(VI-co-VTS) coated on the copper plate were heated both at 380 and 400°C in air for 15 min. FTIR reflection and absorption spectra in the 700–500 cm^{-1} regions of poly(ATS-co-VI) and poly(VI-co-VTS) on copper plates are shown in Figure 10. Due to the increased thermal degradation, two small peaks are observed at 655 and 608 cm^{-1} in spectrum A and these peaks are more outstanding in spectrum B. As shown in spectra C and D, however, poly(VI-co-VTS) shows small copper corrosion peaks at 380°C in air and shows strong corrosion peaks at 400°C. From these results, it can be inferred that poly(VI-co-VTS) shows better corrosion protection capability in comparison with poly(ATS-co-VI) because it can form the thicker siloxane network structure, due to its higher siloxane bond ratio.

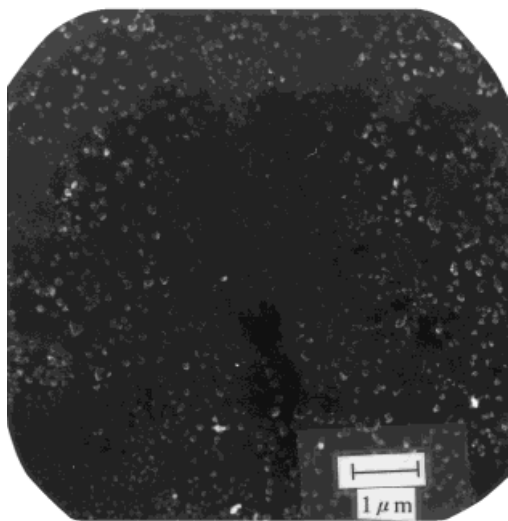
Figure 11 shows scanning electron micrographs of copper surfaces of poly(ATS-co-VI) and poly(VI-co-VTS) heated at 380 and 400°C. In case of poly(ATS-co-VI), cuprous oxide crystals are observed at both 380 and 400°C, but they are the denser in surface density at 400°C. An increase in surface density is due to the increase in the number of film defects because the formation of

Figure 7 Scanning electron micrographs of poly(STS-co-VI) before and after adhesion test: (A) copolymer-coated copper surface before adhesion test; (B) flaked copper surface after adhesion test; (C) the enlarged view of a part in (B); (D) the enlarged view of the b part in (B); (E) the enlarged view of the c part in (B); (F) part flaked off the copper surface.

these oxide crystals is attributed to film defects formed during thermal degradation. In the case of poly(VI-co-VTS), cuprous oxide crystals are not observed at 380°C, but they are observed at 400°C due to the occurrence of film defects by enhanced thermal degradation. These data suggest that the



(A)



(B)

Figure 9 Scanning electron micrographs of poly(γ -MPS-co-VI) heated at 360°C for 15 and 30 min: (A) poly(γ -MPS-co-VI) heated at 360°C for 15 min; (B) poly(γ -MPS-co-VI) heated at 360°C for 30 min.

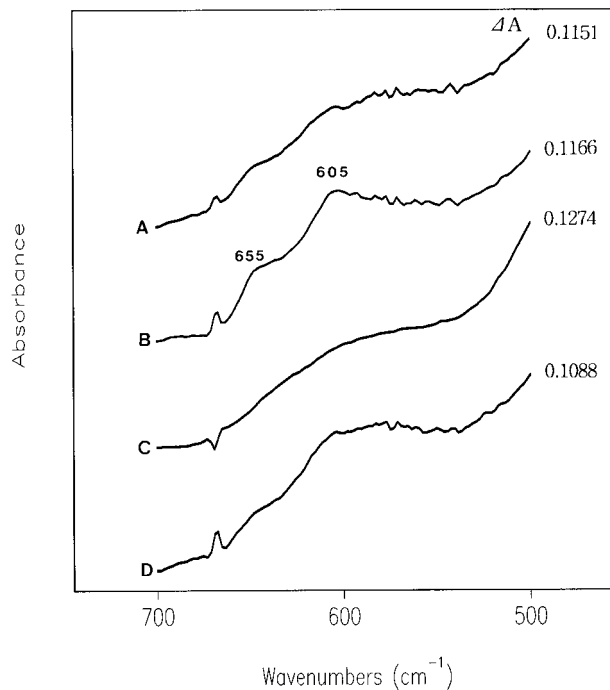


Figure 10 FTIR reflection and absorption spectra of the copolymer films on copper plates: (A) poly(ATS-co-VI) heated at 380°C for 15 min; (B) poly(ATS-co-VI) heated at 400°C for 15 min; (C) poly(VI-co-VTS) heated at 380°C for 15 min; (D) poly(VI-co-VTS) heated at 400°C for 15 min.

surface density of cuprous oxide crystals depends on the number of film defects and that it is higher at 400°C. On the other hand, the number of film defects increases with decreasing thickness of the siloxane network structure produced during heat treatment, which is determined by the heating temperature and siloxane bond ratio. As poly(VI-co-VTS) can form the thicker siloxane network structure due to the higher siloxane bond ratio, it has fewer film defects and the lower surface density of the cuprous oxide crystals. These SEM results are good accordance with the IR results. These copolymer films were not flaked off the copper surface in the adhesion tape test. Table II represents the adhesion test results of the copolymers heated at elevated temperature. In the case of poly(STS-co-VI), most of the coated copolymer film was flaked after the adhesion tape test. However, the other copolymer films were not flaked in spite of corrosion formation through film defects. From the adhesion test, it can be concluded that copolymer films except poly(STS-co-VI) show good interfacial adhesion strength in spite of copolymer degradation and corrosion formation.

Figure 12 shows FTIR reflection and absorp-

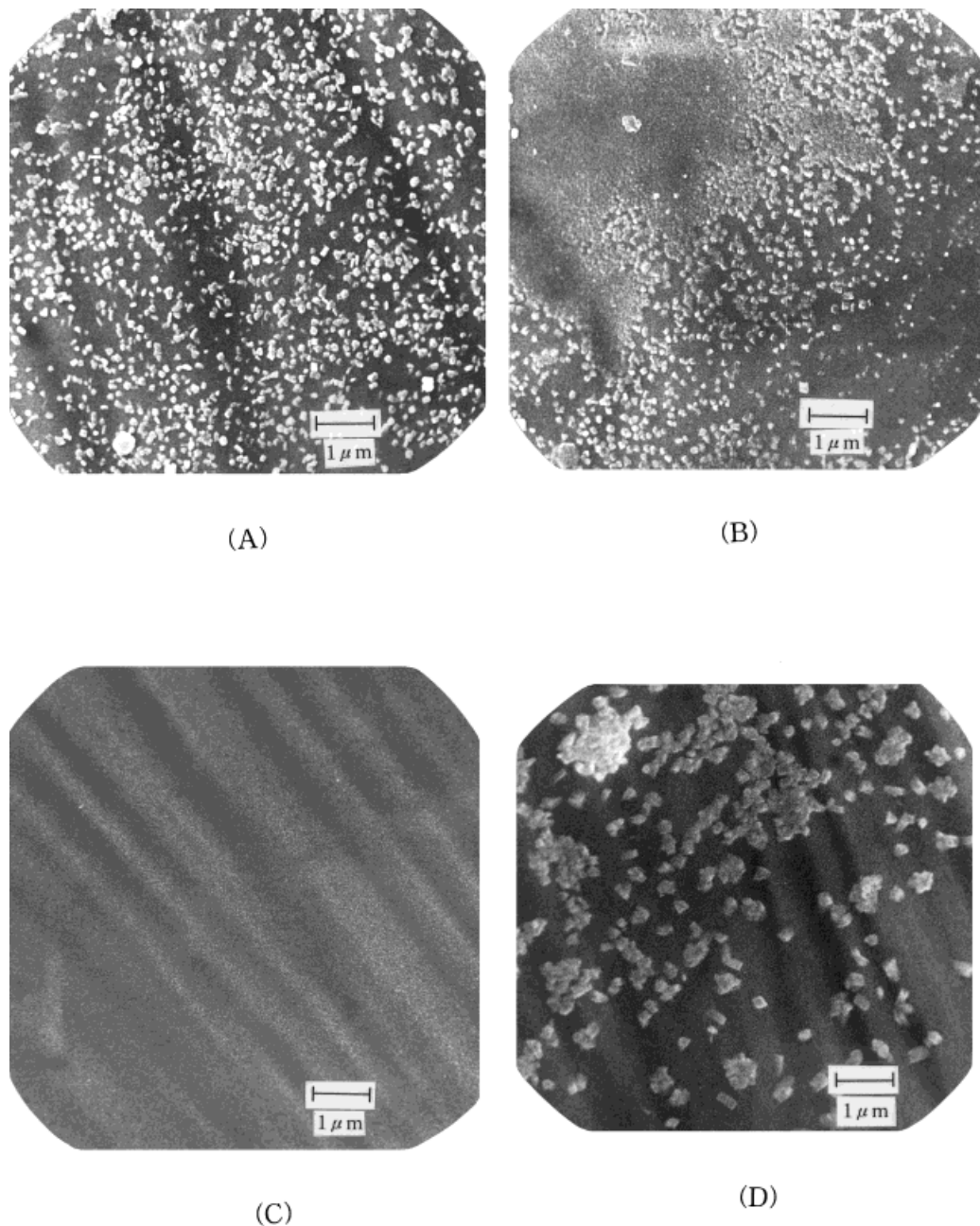


Figure 11 Scanning electron micrographs of the copolymer films on copper plates: (A) poly(ATS-co-VI) heated at 380°C for 15 min; (B) poly(ATS-co-VI) heated at 400°C for 15 min; (C) poly(VI-co-VTS) heated at 380°C for 15 min; (D) poly(VI-co-VTS) heated at 400°C for 15 min.

Table II The Percent Film Flaked After Adhesion Tape Test

Copolymers	poly(STS-co-VI)	poly(γ -MPS-co-VI)	poly(ATS-co-VI)	poly(VI-co-VTS)
Heating condition	360°C for 15 min	360°C for 30 min	400°C for 15 min	400°C for 15 min
% film flaked	95	0	0	0

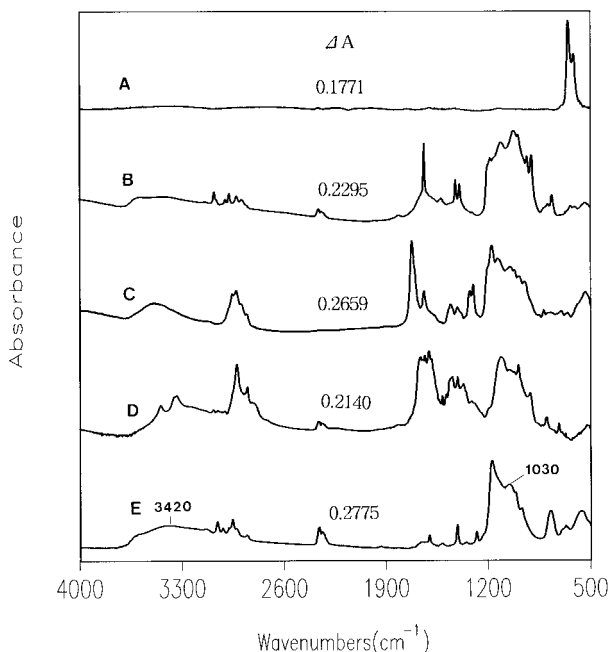


Figure 12 FTIR reflection and absorption spectra of the copolymer films on copper plates heated at 80°C for 24 h in 100% relative humidity condition: (A) bare copper; (B) poly(ATS-co-VI); (C) poly(γ -MPS-co-VI); (D) poly(STS-co-VI); (E) poly(VI-co-VTS).

tion spectra of the copolymer films on copper plates heated in a humid condition. Compared with the spectra in Figure 2, those spectra in Figure 12 show a broader band around 3420 cm^{-1} due to water absorption of the imidazole ring in the copolymer film.¹⁷ In addition, the relative peak intensity at 1030 cm^{-1} increases in the 1300–900 cm^{-1} regions because the hydrolysis of Si—O—CH₃ followed by Si—O—Si bond formation is accelerated by the vaporized water in a humid condition. However, no copolymer degradation is observed in all spectra.

To closely investigate the corrosion formation on the copper surface, Figure 13 concentrates on cuprous oxide peaks in the 700–500 cm^{-1} regions of Figure 12. A bare copper plate shows two corrosion peaks at 655 and 611 cm^{-1} . However, no cuprous oxide peak appears in the spectra of four copolymers. This suggests that a strong chemical bond (Cu—O—Si) exists between the copper surface and the copolymer film and that the Si—O—Cu bond is not debonded by the attack of vaporized water in these experimental conditions. Although poly(STS-co-VI) has the least possibility of forming the Si—O—Cu bond due to having the least Si—O—CH₃, it can successfully sup-

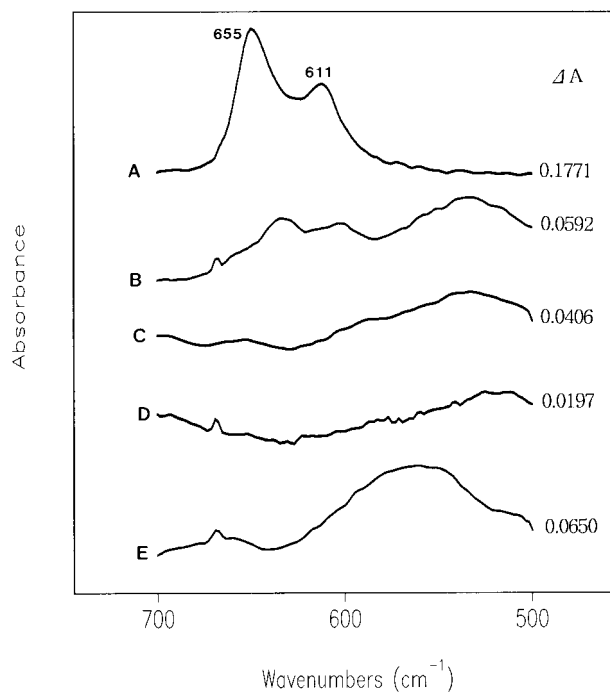


Figure 13 The 700–500 cm^{-1} regions of FTIR reflection and absorption spectra shown in Figure 10: (A) bare copper; (B) poly(ATS-co-VI); (C) poly(γ -MPS-co-VI); (D) poly(STS-co-VI); (E) poly(VI-co-VTS).

press the corrosion formation on the copper surface in this experimental condition.

The possible adhesion formation onto the copper surface of the coated film is represented in Figure 14. The Si—OH group in the silane unit contributes to the adhesion onto the copper surface through chemical bond formation, and the nitrogen atom in the imidazole ring, through the complex bond formation. On the other hand, Si—OH groups not reacting with the copper surface form a Si—O—Si bond with neighboring

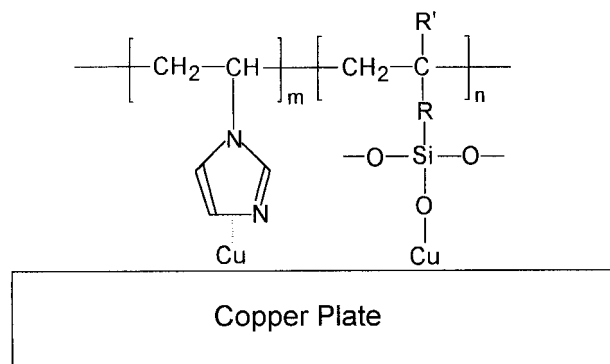


Figure 14 The possible adhesion formation onto copper of silane-modified PVI(1)s.

Si—OH groups. Silane-modified PVI(1)s can protect the copper surface from corrosion formation through these adhesion mechanisms.

CONCLUSION

Four silane-modified PVI(1)s, poly(ATS-co-VI), poly(γ -MPS-co-VI), poly(STS-co-VI), and poly(VI-co-VTS), were synthesized in benzene at 68°C using AIBN as an initiator. All copolymers showed good corrosion protection capability at 80°C with 100% relative humidity. At elevated temperature, however, the corrosion protection capability of silane-modified PVI(1)'s depended on their thermal stability and decreased in the order of poly(VI-co-VTS) > poly(ATS-co-VI) > poly(γ -MPS-co-VI) > poly(STS-co-VI). For poly(STS-co-VI), copper oxide crystals exist not only in the matrix, but also at the copper/copolymer interface. The other copolymers showed the growth of copper oxide crystals through film defects formed during the heat treatment. The adhesion tape test showed that three copolymers, but not poly(STS-co-VI), have good interfacial adhesion strength in spite of cuprous oxide formation through film defects.

REFERENCES

1. C. Taylor and A. Underhill, *J. Chem. Soc. (A)*, **69**, 368 (1969).
2. D. Doonan and A. Balch, *J. Am. Chem. Soc.*, **97**, 1404 (1975).
3. S. Salama and T. Spiro, *J. Am. Chem. Soc.*, **100**, 1105 (1978).
4. M. Mohan, D. Bancroft, and E. Abbett, *Inorg. Chem.*, **18**, 1527 (1979).
5. G. Kolks, C. Frikart, P. Coughlin, and S. Lippard, *Inorg. Chem.*, **20**, 2433 (1981).
6. L. Antolini, L. Battaglia, A. Carradi, G. Marcotrigiano, L. Menabue, G. Pellacani, and M. Saladini, *Inorg. Chem.*, **21**, 1391 (1982).
7. F. Eng and H. Ishida, *J. Mat. Sci.*, **21**, 1561 (1986).
8. F. Eng and H. Ishida, *J. Appl. Polym. Sci.*, **32**, 5021 (1986).
9. F. Eng and H. Ishida, *J. Appl. Polym. Sci.*, **32**, 5035 (1986).
10. S. Yoshida and H. Ishida, *J. Chem. Phys.*, **78**, 6960 (1983).
11. S. Yoshida and H. Ishida, *J. Mat. Sci.*, **19**, 2323 (1984).
12. J. Jang and H. Ishida, *J. Appl. Polym. Sci.*, **49**, 1957 (1993).
13. J. Jang and H. Ishida, *Corros. Sci.*, **33**, 1053 (1992).
14. F. J. Boerio and L. Armogon, *Appl. Spectrosc.*, **32**, 509 (1978).
15. O. Clause, M. Kermaree, L. Bonneviot, F. Villain, and M. Che, *J. Am. Chem. Soc.*, **114**, 4709 (1992).
16. M. Kermaree, J. Y. Carriat, P. Burattin, M. Che, and A. Decarreau, *J. Phys. Chem.*, **98**, 12008 (1994).
17. J. Jang and H. Kim, *J. Appl. Polym. Sci.*, **56**, 1495 (1995).
18. J. Hansen, M. Kumagai, and H. Ishida, *Polymer*, **35**, 4780 (1994).
19. M. Kumagai, K. Tsuchida, Y. Ogino, J. Hansen, and H. Ishida, *Polymer*, **36**, 535 (1995).
20. R. K. Iler, *The Chemistry of Silica*, Wiley, New York, 1979.
21. S. P. Kowalczyk, Y. H. Kim, G. F. Walker, and J. Kim, *Appl. Phys. Lett.*, **52**, 375 (1988).
22. R. M. Tromp, F. Legoues, and P. S. Ho, *J. Vac. Sci. Technol.*, **A3**, 782 (1985).